



13th IEA Heat Pump Conference
April 26-29, 2021 Jeju, Korea

Load-Based Testing Methodology for Evaluating Advanced Heat Pump Control Design

Parveen Dhillon^{a*}, W. Travis Horton^a, James E. Braun^a

^aRay W. Herrick Laboratories, School of Mechanical Engineering, Purdue University, West Lafayette, 47907-2099, USA

Abstract

Optimum control design has been an important aspect of improving the performance, efficiency and thermal comfort delivery of heat pump systems. Despite extensive research work on the development of advanced controls for heat pumps, most heat pump systems in the field still utilize simple controls such as PI (Proportional-Integral), cascaded PI, etc. One of the main reasons for this is the difficulty in assessing the actual improvement in energy performance and thermal comfort delivery of heat pumps with advanced controls. The current practice of performing extensive season-long field studies is time-consuming and requires significant resources to carry out. Also, the performance results of these field studies are limited to the test building type and local climate conditions. To overcome this problem, a load-based testing methodology has been developed to evaluate the performance of advanced heat pump control design for different building types and climate zones in a psychrometric test facility. This methodology provides a way for product developers to significantly accelerate the development of advanced control design and to obtain realistic performance assessments in a timely manner. In this paper, the load-based testing approach is demonstrated for performance assessment of two different control algorithms for a residential heat pump. In addition, the effect of equipment oversizing and undersizing on heat-pump performance is studied utilizing the test approach.

Keywords: Load-based Testing; Performance Evaluation; Control Design; Heat Pump

1. Introduction

In recent years, the increase in microprocessor computing power and decrease in hardware cost have facilitated an opportunity for implementing more advanced controls in heat pump and air-conditioning systems. Even though these improvements lead to more efficient system operation, only a very small fraction of residential air conditioners and heat pumps currently sold in the U.S. market utilize advanced high-efficiency controls [1]. One of the primary reasons for this is the difficulty in evaluating short-term and seasonal performance improvements with advanced controls in a timely and cost-effective manner. To address this issue, a load-based testing methodology has been developed, which allows qualitative and quantitative evaluations of equipment performance with different embedded control designs for representative buildings and climate conditions using tests performed in a laboratory facility. With this methodology, it is also possible to study how equipment performance varies with oversizing or undersizing for a building. The developed methodology can further be used as a basis for seasonal performance ratings of air-conditioning and heat-pumping equipment as presented in [2], [3] and [4].

The load-based testing methodology emulates the response of building sensible and latent loads to the equipment controls in a psychrometric test chamber by continuously updating the room temperature and humidity based on a virtual building model. The test unit thermostat naturally responds to this dynamic temperature variation and controls the equipment in response to a deviation from its setpoint. This method can

* Corresponding author.

E-mail address: dhillonparveen14@gmail.com

capture realistic performance of a heat pump in a psychrometric test chamber, similar to a field application. In this way, load-based testing can be implemented to quantify performance differences among different equipment control architectures in a lab-setup and also qualitatively study the dynamic performance and comfort delivery of the equipment. This testing methodology can be applied to both variable-speed as well as staged equipment.

The method is based on an approach presented by Hjortland & Braun [5] for performance characterization of fixed-speed and variable-speed unitary air-conditioning equipment. Patil *et. al.* [2] and Cheng *et. al.* [6] applied the load-based testing methodology to generate data for estimating seasonal performance of variable-speed residential heat pumping and air conditioning equipment. In the current paper, the load-based testing methodology is implemented to perform a qualitative and quantitative comparison of the dynamic performance of a variable-speed heat pump in cooling mode in terms of energy efficiency and comfort delivery. The impact of two different control modes is considered along with equipment undersizing and oversizing.

To capture the dynamic performance of equipment that is representative of field applications with this methodology, it is important to have a representative virtual building model and representative outdoor ambient conditions. Also, to allow for testing different size heat pumps, the virtual building model needs to be scalable with equipment rated capacity. In this study, the load-based testing methodology was implemented on a 5-ton residential heat pump with an appropriately scaled virtual building model. The study considered only cooling mode performance for typical mid-summer and peak-summer season days with representative daily outdoor temperature profiles.

2. Load-Based Testing Overview

The load-based testing methodology captures the holistic performance of an equipment including its thermostat and integrated controls in a test facility setup. Fig. 1 outlines the layout of the load-based test approach of a split-type heat pump system installed in two side-by-side psychrometric chambers.

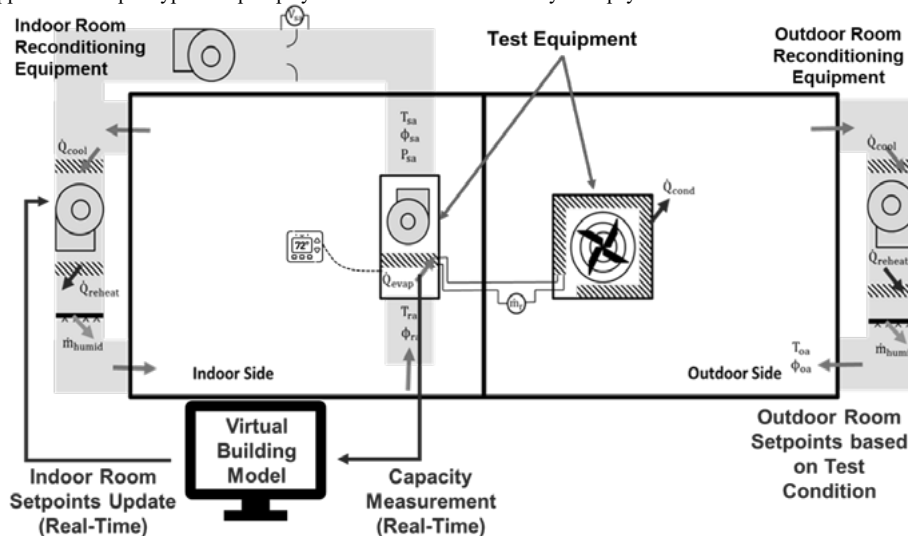


Fig. 1. Load-Based Testing Schematic of a Split-type Heat Pump System

As shown in Fig. 1, in this methodology, the equipment capacity is measured in real-time and fed into a virtual building model. The virtual building model estimates the building load based on the current indoor and outdoor conditions. Then, based on the difference in the equipment capacity and building load, the virtual building temperature and humidity are updated according to the virtual building thermal and moisture dynamics. The updated virtual building conditions are then provided as setpoints to the indoor psychrometric room reconditioning system. In this way, the response of a virtual building is emulated in the indoor-side test room. The outdoor test room conditions are varied according to a representative temperature profile according to climate and season.

In cooling mode tests, when the equipment sensible capacity is more than the sensible building load, the indoor room temperature decreases; whereas, the indoor room temperature increases when the capacity is lower than the load. Similarly, the indoor room humidity varies based on the virtual building latent load and the equipment latent capacity. The test unit thermostat senses this dynamic variation of indoor space temperature and humidity, and to maintain the indoor conditions to the thermostat setpoint, the equipment responds to this variation based on its integrated controls. This enables the load-based testing methodology to capture an overall dynamic performance of equipment that is representative of a field application.

The virtual building model can be defined based on the desired complexity of the representative building for the underlining experimental study. Hjortland & Braun [5] and Patil *et. al.* [2] described a virtual building model for a representative residential building that was employed for the experimental study presented here.

The virtual building model calculates the building sensible heat gain to the air or load scaled according to the equipment rated sensible capacity ($\dot{Q}_{cool,s,D}$) at design conditions as per the equation (1).

$$\dot{Q}_{load,s} = \frac{1}{F} \cdot \frac{\dot{Q}_{cool,s,D}}{(T_{OD,D} - T_{Bal,D})} \cdot (T_{OD} - T_{Bal}) \quad (1)$$

where the building-load sizing factor (F) is used to scale the building load, based on the equipment sizing for a building. For example, for the case of F equal to 1.25 which makes $1/F$ 0.8 i.e. building load which the equipment meets is 80% of the load for which equipment is designed, so in this case, the equipment is 20% oversized. The effective balance point temperature (T_{Bal}) is updated according to equation (2) based on the current indoor temperature (T_{ID}) and the indoor target temperature ($T_{ID,SP}$) which is also the equipment thermostat temperature setpoint. This formulation accounts for the change in building load due to variations in the indoor temperature from its design conditions.

$$T_{Bal} = T_{Bal,D} + (T_{ID} - T_{ID,SP}) \quad (2)$$

The virtual building latent energy gain or load is calculated using a constant sensible heat ratio model for the representative building as per equation (3).

$$\dot{Q}_{load,l} = \dot{Q}_{load,s} \cdot \left(\frac{1}{SHR_{building}} - 1 \right) \quad (3)$$

Then based on the virtual building loads and equipment measured capacities, the virtual building temperature and humidity ratio are updated for the next time step as per equation (4) and (5), which are supplied as the indoor test room setpoints that are controlled by the reconditioning system.

$$T_{ID}(t + \Delta t) = T_{ID}(t) + \Delta t \cdot \left(\frac{\dot{Q}_{load,s} - \dot{Q}_{cool,s}}{C_s} \right) \quad (4)$$

$$\omega_{ID}(t + \Delta t) = \omega_{ID}(t) + \Delta t \cdot \left(\frac{\dot{Q}_{load,l} - \dot{Q}_{cool,l}}{h_{fg} \cdot C_w} \right) \quad (5)$$

where the sensible (C_s) and moisture (C_w) capacitances for a representative residential building are scaled with the equipment capacities at design conditions using equation (6) and (7) respectively.

$$C_s [J/^\circ F] = \frac{\dot{Q}_{cool,s,D} [W] \cdot 150 [s]}{\Delta T_{tstat,db} [^\circ F]} \quad (6)$$

$$C_w [kg] = \frac{\dot{Q}_{cool,D} [W]}{12.9 [W/kg]} \quad (7)$$

Based on the equations (1)-(7), the virtual building model continuously controls the indoor test room conditions to emulate the response of a representative building to the equipment performance. The first step in

load-based testing is to measure the equipment rated sensible and latent capacity at design conditions and use them to scale the virtual building parameters. This measurement is done using a steady-state test with constant indoor and outdoor test room conditions and the equipment running at maximum capacity.

3. Experimental Method

For each test, the outdoor temperature is varied according to a typical daily temperature profile for the season considered. For a representative mid-summer day, the outdoor temperature is varied between 65°F (18.33°C) and 85°F (29.45°C). For a peak-summer day, the outdoor temperature is varied between 85°F (29.45°C) and 105°F (40.56°C). The representative hourly outdoor temperature profiles were generated based on Erbs *et. al.* [7] and Mitchell & Braun [8] as per equation (8).

$$T_{OD} = \left(T_{OD,max} - \frac{(T_{OD,max} - T_{OD,min})}{2} \right) + (T_{OD,max} - T_{OD,min}) \cdot [0.4632 \cos(\tau - 3.8051) + 0.0984 \cos(2\tau - 0.360) + 0.0168 \cos(3\tau - 0.822) + 0.0138 \cos(4\tau - 3.513)] \quad (8)$$

where,

$$\tau = \frac{2\pi(2.4 \cdot t - 1)}{24}; t: \text{time of day in hours} \quad (9)$$

Equation (9) was modified to compress the complete daily temperature change from 24 hours to 10 hours to accelerate the testing. This is reasonable because the dynamic response of the equipment with its integrated controls is still orders of magnitude faster than the dynamic variation of the outdoor temperature. Fig. 2 shows the derived typical outdoor temperature profile for the emulated mid-summer and peak-summer days.

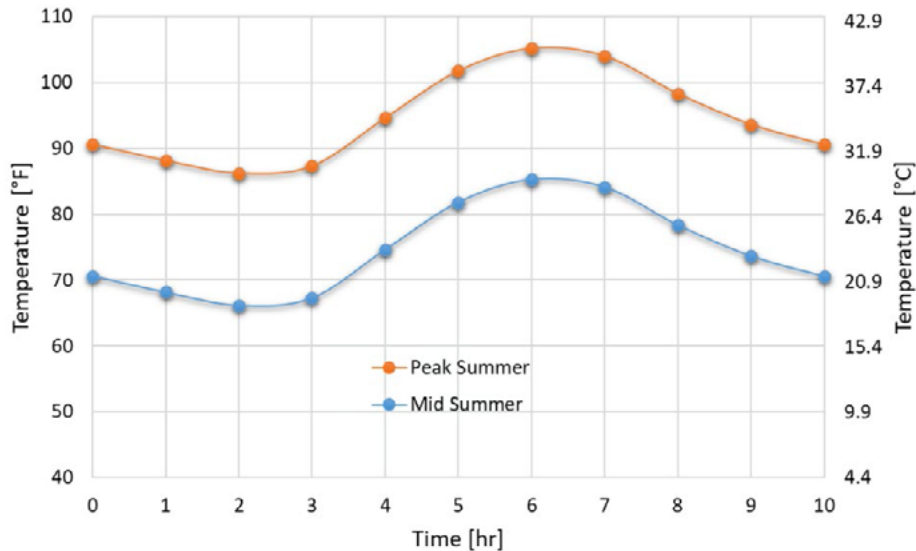


Fig. 2. Representative Outdoor Temperature Profile for Mid-Summer and Peak-Summer Day

The equipment was tested with two different control modes: A and B; three different equipment sizing scenarios: nominal, undersizing and oversizing; and for the two representative cooling season days: mid-summer and peak-summer. Table 1 outlines the test matrix for the experimental study conducted in this paper.

Table 1. Test Matrix for the Experimental Study of the Heat-Pump

Test	Cooling Season Day	Equipment Sizing	Control Mode
0	Baseline Steady-State Test at Design Conditions		
1	Peak-Summer	Nominal	A
3	Peak-Summer	Nominal	B
2	Mid-Summer	Nominal	A
4	Mid-Summer	Nominal	B
5	Mid-Summer	Oversize (20%)	A
6	Mid-Summer	Oversize (20%)	B
7	Peak-Summer	Oversize (20%)	B
8	Mid-Summer	Undersize (20%)	A
9	Mid-Summer	Undersize (20%)	B
10	Peak-Summer	Undersize (20%)	B

To scale the virtual building parameters for the heat-pump under investigation, first, rated capacity is measured through a baseline steady-state test conducted at the cooling design conditions (Table 2) using a thermostat setpoint such that the equipment provided maximum cooling capacity.

Table 2. Cooling Design Conditions

Indoor Conditions		Outdoor Conditions
Temperature	Relative Humidity	Temperature
75°F (23.8°C)	50%	95°F (35°C)

Based on the equipment performance at design conditions, the virtual building parameters were derived for the heat pump being studied as shown in Table 3.

Table 3. Virtual Building Parameters

Parameter	F			$\dot{Q}_{cool,s,d}$	$\dot{Q}_{cool,d}$	$T_{OD,D}$	$T_{Bal,D}$
	Nominal	Oversize (20%)	Undersize (20%)	W	W	°F (°C)	°F (°C)
Value	1	1.25	0.83	12850.6	15192.6	95 (35)	62 (16.6)
Parameter	$T_{ID,SP}$	$RH_{ID,SP}$	C_s	C_w	$\Delta T_{estat,db}$	$SHR_{building}$	Δt
	°F (°C)	%	J/°F (J/°C)	kg	°F (°C)	-	second
Value	75(23.8)	50	1927596 (1070887)	1177.7	1 (0.56)	0.8	1

For each test, the first two hours were used as a warm-up period for the equipment. In these two hours, the outdoor temperature was kept constant to the 2nd hour temperature (Fig. 2); and indoor conditions were kept constant at target comfort conditions of 75°F (23.8°C) and 50% RH. Following this, the outdoor room temperature varied according to the defined temperature profile from the 2nd to 10th hour (Fig. 2). During these tests, the indoor temperature and humidity setpoints for the reconditioning system were updated continuously according to the virtual building model response, as outlined in section 2, utilizing the parameters from Table 3. In this way, the equipment dynamic performance was captured for an 8-hour test duration. The test unit performance results were analyzed only for this 8-hour duration when the outdoor temperature was varying. The results are presented in section 5.

In order to compare comfort delivery for the different strategies during cooling load-based tests, comfort violation limits were defined. Based on [9], a temperature limit of 2°F higher than the target indoor temperature setpoint, i.e. 77°F, was established. In addition, relative humidity of 10% higher than a target indoor relative humidity setpoint, i.e. 60%, was selected. The total time-duration that the heat-pump failed to maintain these limits was determined for temperature and humidity comfort individually and used as a measure of discomfort.

4. Test Setup Layout

The load-based testing was implemented at Purdue University on a split-type heat-pump system using two side-by-side psychrometric test chambers at the Ray W. Herrick Laboratories. Fig. 1 shows the layout of the system installation in the test facility, along with an outline for controlling the indoor and outdoor test room conditions during dynamic testing. Fig. 3 illustrates the schematic of the heat pump system along with the air, refrigerant, and power side measurements. The heat-pump was installed in the test rooms based on ASHRAE guidelines for performance measurement as outlined in [10], [11], [12], [13], [14], [15] and [16]. The indoor unit return and supply air temperatures were measured using a thermocouple grid, and humidities were measured using a chilled mirror dew point hygrometer. The indoor unit supply air volumetric airflow was measured using a nozzle box code-tester that was used to calculate the air-side sensible and latent capacity with the air-enthalpy method. To verify the air-side measurements, refrigerant side capacity was also measured. For this, refrigerant mass flow rate was measured using a Coriolis-effect based mass flow meter installed in the liquid line. In addition, pressure and temperature sensors were installed to measure the refrigerant side properties at different state points of the cycle as shown in Fig. 3. Furthermore, two power-meters were installed to measure the indoor and outdoor unit power consumption.

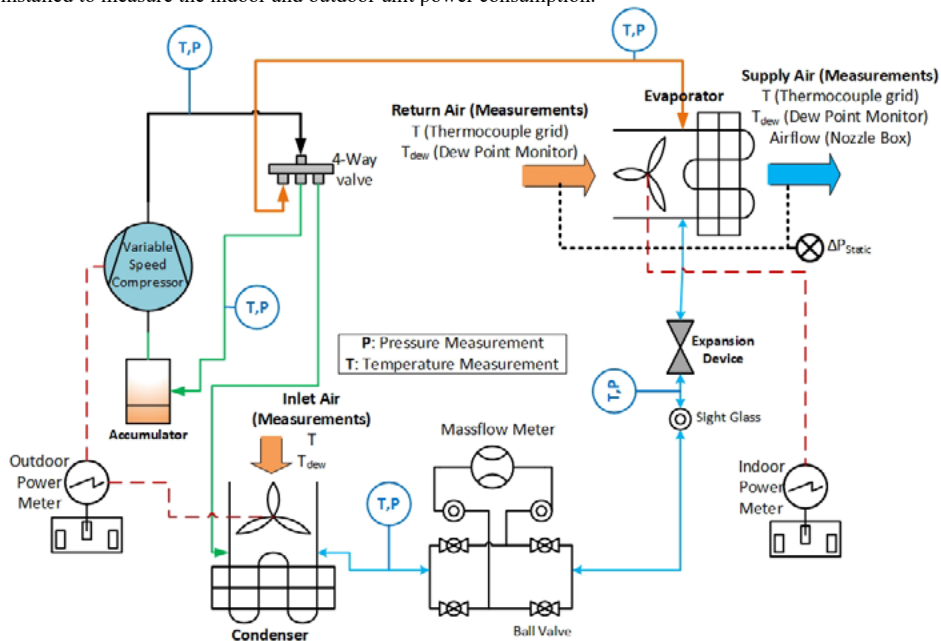


Fig. 3. Test Heat-Pump Schematic with the Air, Refrigerant, and Power Side Measurements

5. Results

Fig. 4 presents the performance of the heat pump for 8-hour dynamic test duration on a typical mid-summer day with nominal equipment sizing for control mode A. The upper subplot shows the equipment performance variation with time, including the virtual building load (sensible and latent), the heat-pump capacity (sensible and latent), and the equipment total power consumption. The lower subplot illustrates the virtual building and test rooms temperature and relative humidity variation for the test duration. In the lower subplot, the left vertical axis corresponds to the indoor virtual building (dotted line) and indoor test room (solid line) temperature and relative humidity; whereas, the right vertical axis corresponds to outdoor temperature variation.

As can be seen from Fig. 4, the virtual building outdoor temperature changed between 65°F and 85°F for this representative mid-summer day. When the heat-pump cycled on/off, the outdoor temperature fluctuated around the setpoint (Virtual Building ODT) which is due to the sudden changes in capacity requirement from

the test room reconditioning system. This could be overcome by fine-tuning the test room controller gains and updating architecture, but for this study, these modifications were not implemented due to time constraints.

The test unit thermostat was set at the target comfort conditions of 75°F (black dotted line); however, for this equipment, there is no provision to set a target humidity setpoint. Subsequently, the indoor temperature and humidity varied based on the interaction of the equipment thermostat controls with the virtual building load. When the building sensible load (red dotted line) is higher than the equipment sensible capacity (green solid line), the indoor temperature (blue solid line) increases; whereas, when the heat-pump sensible capacity is higher than the building sensible load, the indoor temperature decreases. Similarly, the indoor humidity varies based on the difference in the latent load (orange dotted line) and the latent capacity (sky-blue solid line).

In this test, the virtual building indoor temperature varied between 71°F and 76.4°F, and relative humidity varied between 49.7% to 64%. For moderate day, this variable-speed equipment cycled on and off throughout the day based on the thermostat interaction with the changing indoor temperature and demonstrated a behavior effectively similar to a single-stage system. As the outdoor temperature increased, correspondingly, the building load increased and to compensate for this higher load, the heat-pump run-time fraction for a cycle increased. The equipment was able to maintain the indoor temperature within comfort levels (<77°F) for the complete duration of the test; however, it failed to maintain the humidity within the comfort limit (<60%) for some duration around the 2nd hour and towards the end from the 7th hour onwards. Also, Fig. 4 reveals that the system maintained the indoor temperature below the thermostat setpoint for most of the time and the indoor temperature variation band was larger than $\pm 1^\circ\text{F}$ around the thermostat setpoint, which might be due to its inbuilt offset and dynamics. These results illustrate the ability of the test methodology to capture the dynamic interaction of the equipment, its controls, and the building load. On a side note, the building load does not follow the exact profile as of the outdoor temperature variation, because of the dependence of building load on indoor temperature deviations from its target design conditions.

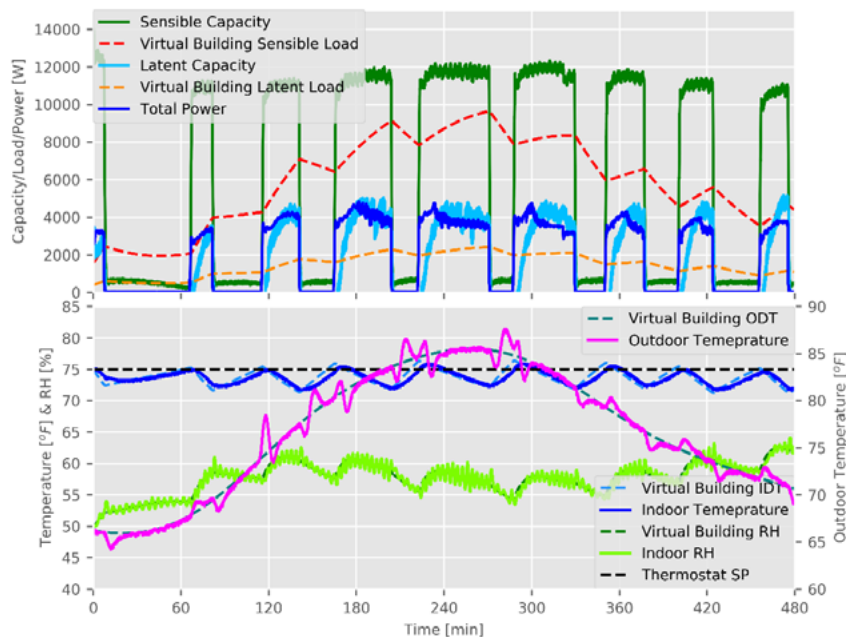


Fig. 4. Equipment Dynamic Performance on a Mid-summer Day with Nominal Equipment Sizing and Control Mode A

Fig. 5 presents the equipment performance for a peak-summer day with control mode A and nominal equipment sizing. Initially, when the ambient temperature was relatively low, the heat-pump cycled on/off and was able to maintain the indoor temperature around its setpoint; however, as the outdoor temperature increased, the equipment ran at full capacity and failed to compensate for the larger building load leading to indoor temperatures that rose above the comfort limits. However, the equipment was able to maintain the relative

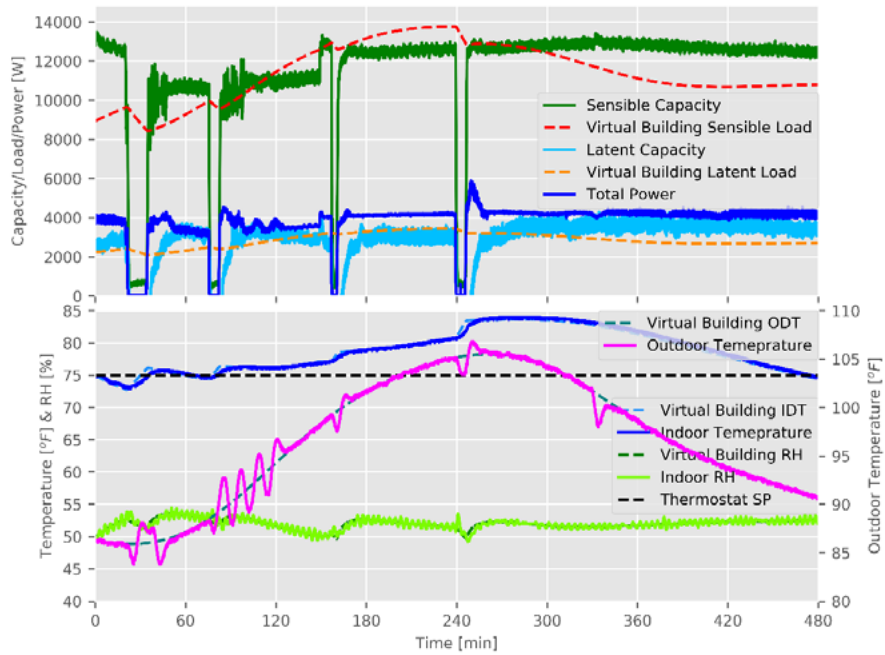


Fig. 5. Equipment Dynamic Performance on a Peak-summer Day with Nominal Equipment Sizing and Control Mode A

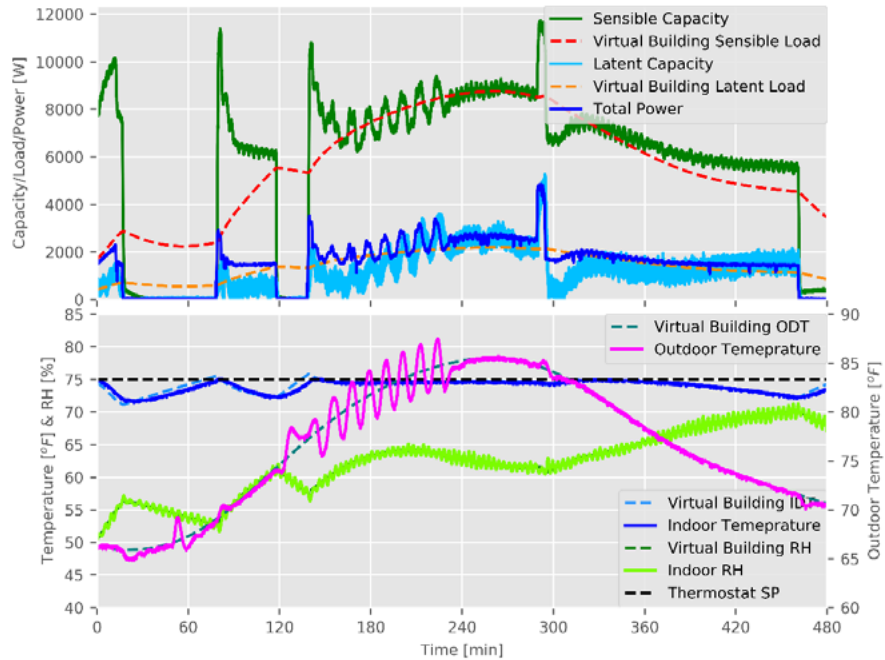


Fig. 6. Equipment Dynamic Performance on a Mid-summer Day with Nominal Equipment Sizing and Control Mode B

humidity within comfort limits, which can be attributed to a smaller sensible heat ratio of the evaporator coil at full compressor speed. These results illustrate the consequences of not properly sizing the equipment for the design conditions. The other interesting observation is that the equipment cycled off at some conditions even when the indoor temperature was well above the thermostat setpoint, which might be due to some inbuilt features in the equipment controls. These types of control issues and their impact on performance can be identified in the laboratory through load-based testing prior to deployment in the field.

The heat-pump performance was also evaluated with a 2nd controller design (control mode B). Fig. 6 shows the results of a test with control mode B for a mid-summer day and nominal equipment sizing. At the start, when the outdoor temperature was low i.e. the building load was low, the equipment cycled on/off similar to the case of control mode A (Fig. 4), although with lower power consumption and longer cycle duration compared to control mode A. Next, as the outdoor temperature increased the system ran continuously in variable speed mode rather than cycling on/off as with control mode A. Then the system cycled off again at low ambient temperature towards the end. The equipment was able to maintain the indoor temperature steadily around the thermostat setpoint instead of oscillating around the setpoint as occurred with control mode A (Fig. 4). However, in this control mode B, the heat-pump failed considerably to keep the indoor humidity within comfort levels compared to control mode A. These results illustrate the usefulness of the load-based test approach in comparing the dynamic performance and comfort delivery of a system with different controller designs.

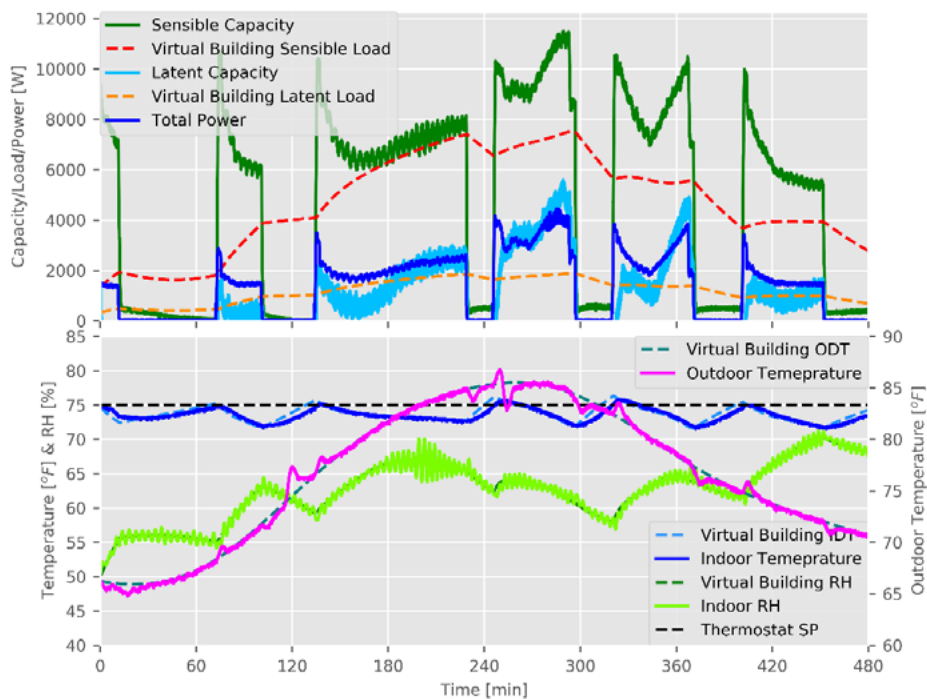


Fig. 7. Equipment Dynamic Performance on a Mid-summer Day with Equipment Oversizing and Control Mode B

Heat-pump performance was also evaluated for the case of equipment oversizing and undersizing. Fig. 7 and Fig. 8 illustrate the test results for the equipment oversizing and undersizing cases respectively, for a mid-summer day with control mode B. In the case of equipment oversizing (Fig. 7), where the building load was smaller compared to nominal sizing for the same ambient conditions, the equipment cycled on/off during the entire time, in contrast to the continuous operation in case of nominal sizing (Fig. 6). For equipment undersizing (Fig. 8), where building load was higher compared to nominal sizing, the heat-pump ran continuously for most of the time, similar to nominal sizing case (Fig. 6), but with higher power consumption to compensate for the larger building load. As observed earlier, when equipment is cycling on/off, as in case

of oversizing, the indoor temperature oscillations are relatively large around the thermostat setpoint, which can be uncomfortable for occupants; whereas, in the undersizing case with continuous equipment operation, the system was able to maintain indoor temperature more steadily around the setpoint. Nonetheless, with control mode B, the equipment was not able to provide humidity comfort for both the undersizing and oversizing cases.

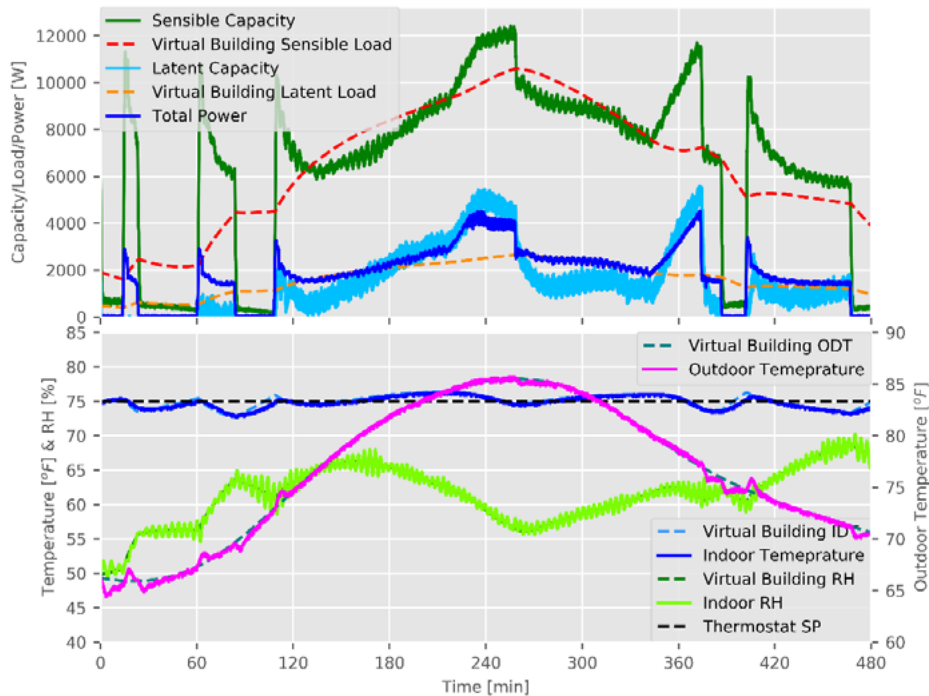


Fig. 8. Equipment Dynamic Performance on a Mid-summer Day with Equipment Undersizing and Control Mode B

Table 4 and Table 5 show overall performance results for the 10 different combination cases of the season (mid-summer & peak-summer), equipment sizing (nominal, oversize, & undersize) and control mode (A & B). Table 4 presents the integrated equipment capacity, building load, power consumption, and COP for the 8-hour dynamic load-based tests. For the same season and equipment sizing scenario, the integrated virtual building sensible and latent loads are comparable for both control modes. There is a slight difference, because with different control modes, the indoor temperature varies differently, which then propagates to the building load. The results show that as the ambient temperature increases in peak-summer season, the system average COP decreases. Furthermore, with the same ambient conditions and equipment sizing, the system performs more efficiently with control mode B. In addition, for mid-summer season, with control mode A, the equipment efficiency improves with oversizing and worsens with undersizing; whereas, the contrary happens with control mode B.

Table 5 summarizes the comfort delivery performance of the equipment for the different tests. It indicates the total number of hours, out of the 8-hour test duration, that the system is not able to maintain the indoor temperature and humidity within comfort limits for cooling, which were 77°F for temperature and 60% for relative humidity. Table 5 also shows the minimum and maximum virtual building temperature and relative humidity for each test. The system failed to maintain the temperature comfort for most of the peak-summer season tests. This was particularly extreme at high load periods with equipment undersizing. In the mid-summer season, even though the temperature comfort levels were mostly maintained, the humidity comfort was violated in both control mode A and B for all three equipment sizing scenarios. In addition, the humidity comfort violation duration with control mode B was more than twice the period in case of control mode A. So, although the control mode B is better from an energy consumption perspective, humidity comfort is sacrificed.

Table 4. Building Load, Cooling Rate, and Power Consumption Performance Results

Test	Season	Equipment Sizing	Control Mode	Virtual Building Sensible Load	Sensible Capacity	Virtual Building Latent Load	Latent Capacity	Power Consumption	System COP
				Integrated					Average
				kWh	kWh	kWh	kWh	kWh	-
1	Peak-Summer	Nominal	A	89.02	90.95	22.25	21.70	29.88	3.77
2	Peak-Summer	Nominal	B	91.66	93.43	22.91	21.35	29.34	3.91
3	Mid-Summer	Nominal	A	41.13	49.25	10.28	9.89	14.95	3.96
4	Mid-Summer	Nominal	B	40.35	44.17	10.09	8.30	11.40	4.60
5	Mid-Summer	Oversize (20%)	A	31.97	41.04	7.99	8.13	12.90	3.81
6	Mid-Summer	Oversize (20%)	B	32.51	38.47	8.13	6.09	10.54	4.23
7	Peak-Summer	Oversize (20%)	B	76.66	79.72	19.16	17.86	27.46	3.55
8	Mid-Summer	Undersize (20%)	A	42.90	52.77	10.73	10.88	15.86	4.01
9	Mid-Summer	Undersize (20%)	B	44.67	51.87	11.17	10.00	13.89	4.46
10	Peak-Summer	Undersize (20%)	B	97.66	92.97	24.41	20.09	29.38	3.85

Table 5. Comfort Delivery Performance Results

Test	Season	Equipment Sizing	Control Mode	Temperature Comfort Violation	Humidity Comfort Violation	Virtual Building Temperature		Virtual Building Relative Humidity	
				Total	Total	Min	Max	Min	Max
				Hour	Hour	°F	°F	%	%
1	Peak-Summer	Nominal	A	4.28	0.00	72.7	83.6	49.7	53.5
2	Peak-Summer	Nominal	B	3.64	0.00	73.3	81.6	49.8	59.9
3	Mid-Summer	Nominal	A	0.00	2.38	71.0	76.4	49.7	64.0
4	Mid-Summer	Nominal	B	0.00	6.36	71.1	75.8	49.8	70.1
5	Mid-Summer	Oversize (20%)	A	0.00	3.48	71.2	76.8	49.9	65.5
6	Mid-Summer	Oversize (20%)	B	0.00	6.86	71.1	76.3	49.8	71.5
7	Peak-Summer	Oversize (20%)	B	0.12	0.62	72.1	77.4	50.0	60.7
8	Mid-Summer	Undersize (20%)	A	0.19	2.43	71.4	77.6	49.4	65.8
9	Mid-Summer	Undersize (20%)	B	0.00	6.25	72.7	76.3	49.7	69.5
10	Peak-Summer	Undersize (20%)	B	5.45	0.00	75.0	86.2	49.2	57.1

6. Summary and Conclusions

This paper presents the application of a new load-based testing methodology for evaluating the dynamic performance of a residential heat-pump system under conditions that are similar to a field application. First, an overview of the approach was provided along with a representative residential virtual building mathematical model, followed by the experimental study method and the representative outdoor ambient conditions for this investigation. Testing of the heat-pump was limited to cooling mode and equipment dynamic performance was measured for various scenarios based on a combination of two different representative summer days, two different control modes, and three distinct equipment sizing situations. The results illustrate the benefits of load-based testing in assessing the qualitative and quantitative effect of different ambient conditions, control design, and equipment sizing on the equipment performance from efficiency as well as comfort perspective. For example, one of the control modes was observed to be more energy efficient but failed to maintain indoor humidity comfort levels. In this way, the methodology provides a way to evaluate realistic equipment dynamic performance in a test-facility environment much more quickly and at a much lower cost than would be possible

for field testing. The methodology can be readily used for different building types and climate locations of interest by updating the virtual building model and ambient conditions accordingly. This can be advantageous in accelerating the development and assessment of advanced controls, diagnostics, and other features.

7. Nomenclature

Variable	Description	Variable	Description
$\dot{Q}_{load,s}$	ing sensible load [W]	F	building load sizing factor [-]
$\dot{Q}_{cool,s,D}$	equipment design sensible capacity [W]	$T_{OD,D}$	the outdoor dry-bulb temperature at design condition [°C]
$T_{Bal,D}$	n balance point temperature [°C]	T_{OD}	outdoor dry-bulb temperature [°C]
T_{Bat}	effective balance point temperature [°C]	T_{ID}	virtual building indoor dry-bulb temperature [°C]
$T_{ID,SP}$	indoor temperature comfort condition (test unit thermostat setpoint) [°C]	$RH_{ID,SP}$	target indoor humidity comfort condition (test unit thermostat setpoint) [%]
$\dot{Q}_{load,l}$	ing latent load [W]	Δt	update time-step [s]
ω_{ID}	il building indoor humidity ratio [kg _{water} /kg _{dryair}]	h_{fg}	the heat of vaporization of water [J/kg]
$\dot{Q}_{cool,s}$	ment sensible cooling capacity [W]	$\dot{Q}_{cool,l}$	equipment latent cooling capacity [W]
C_s	il building sensible capacitance [J/°C]	C_w	virtual building moisture capacitance [kg]
$\Delta T_{stat,db}$	ostat deadband [°C]	$\dot{Q}_{cool,D}$	equipment design total capacity [W]
RH	relative humidity [%]	$SHR_{building}$	building sensible heat ratio [-]
COP	coefficient of performance [-]	IDT	indoor temperature [°C or °F]

Acknowledgments

The authors would like to acknowledge the Herrick Lab's engineering technician - Frank Lee, research associate - Orkan Kurtulus, and graduate students - Vatsal Shah, Weigang Hou, and Jie Ma, for their help in the experiment work.

References

- [1] ACEEE, "2019 Efficiency Programs : Promoting High- Efficiency Residential Air Conditioners and Heat Pumps," *ACEEE*, 2019.
- [2] A. Patil, A. L. Hjortland, L. Cheng, P. Dhillon, J. E. Braun, and W. T. Horton, "Load-based Testing to Characterize the Performance of Variable-Speed Equipment," 2018, [Online]. Available: <https://docs.lib.purdue.edu/iracc/2076>.
- [3] P. Dhillon, A. Patil, L. Cheng, J. E. Braun, and W. T. Horton, "Performance Evaluation of Heat Pump Systems Based on a Load-based Testing Methodology," 2018, [Online]. Available: <https://docs.lib.purdue.edu/iracc/2077>.
- [4] CSA, *CSA EXP07:19 Load-based and climate-specific testing and rating procedures for heat pumps and air conditioners*. 2019.
- [5] A. L. Hjortland and J. E. Braun, "Load-based testing methodology for fixed-speed and variable-speed unitary air conditioning equipment," *Sci. Technol. Built Environ.*, vol. 25, no. 2, pp. 233–244, 2019, doi: 10.1080/23744731.2018.1520564.
- [6] L. Cheng, P. Dhillon, W. T. Horton, and J. E. Braun, "Automated laboratory load-based testing and performance rating of residential cooling equipment," *Int. J. Refrig.*, vol. 123, pp. 124–137, 2021, doi: 10.1016/j.jrefrig.2020.11.016.
- [7] D. G. Erbs, W. A. Beckman, and S. A. Klein, "Estimation of degree-days and ambient temperature bin data from monthly-average temperatures," *ASHRAE J.*; (*United States*), 1983.
- [8] J. W. Mitchell and J. E. Braun, *Principles of heating, ventilation, and air conditioning in buildings*. John Wiley & Sons, 2012.
- [9] A. ASHRAE, "Standard 55-2017 Thermal environmental conditions for human occupancy," *ASHRAE Stand.*, 2017.
- [10] ASHRAE, "ANSI/ASHRAE Standard 37-2009 (RA 2019). Methods of Testing for Rating Electrically Driven Unitary Air-Conditioning and Heat Pump Equipment." ASHRAE, 2019.
- [11] ASHRAE, "ANSI/ASHRAE Standard 41.1-2013. Standard Method for Temperature Measurement." ASHRAE, 2013.
- [12] ASHRAE, "ANSI/ASHRAE Standard 41.6-2014. Standard Method for Humidity Measurement." ASHRAE, 2014.
- [13] ASHRAE, "ANSI/ASHRAE Standard 41.2-2018. Standard Methods for Air Velocity and Airflow Measurement." ASHRAE, 2018.
- [14] ASHRAE, "ANSI/ASHRAE Standard 41.10-2013. Standard Methods for Refrigerant Mass Flow Measurement Using Flowmeters." ASHRAE, 2013.
- [15] ASHRAE, "ANSI/ASHRAE Standard 41.3-2014. Standard Methods for Pressure Measurement." ASHRAE, 2014.
- [16] ASHRAE, "ANSI/ASHRAE Standard 41.11-2014. Standard Methods for Power Measurement." ASHRAE, 2014.